

Initial Observation and Analysis of Dielectric-Charging Effects on RF MEMS Capacitive Switches

Xiaobin Yuan, *Student Member, IEEE*, Sergey Cherepko, *Student Member, IEEE*, James Hwang, *Fellow, IEEE*, Charles L. Goldsmith, *Senior Member, IEEE*, Christopher Nordquist, *Member, IEEE* and Christopher Dyck, *Member, IEEE*.

Abstract—Capacitance-voltage and RF-output characteristics of electrostatically actuated MEMS switches were measured under different control and stress voltages. It was found that positive voltage stress caused negative charging of the dielectric whereas negative voltage stress caused positive charging of the dielectric. This is consistent with the amphoteric nature of traps in the silicon oxynitride dielectric used for the switches. A hypothesis of charge injection in minutes and charge migration in milliseconds was proposed to explain real-time and non-symmetrical drift of pull-down and hold-down voltages of the switches.

Index Terms—RF, MEMS, switch, dielectric, charging, trap.

I. INTRODUCTION

Despite the attractive performance characteristics of RF MEMS switches, their commercialization is hindered by a number of factors such as reliability and packaging cost. In particular, electrostatically actuated RF MEMS capacitive switches can be affected by dielectric-charging effects such as control-voltage drift and stiction [1]. The dielectric is typically silicon dioxide or nitride formed by plasma-enhanced chemical vapor deposition (PECVD) with a high density ($\sim 10^{18}/\text{cm}^3$) of traps associated with silicon dangling bonds [2]. The traps are amphoteric so they can be either positively or negatively charged. During switch operation, the electric field across the dielectric can be of the order of 10^6 V/cm causing electrons or holes to be injected into the dielectric and become trapped. With repeated operation, charge gradually builds up in the dielectric resulting in control-voltage drift or stiction [1].

Summary submitted on February 27, 2004.

X. Yuan, S. V. Cherepko and J. C. M. Hwang are with Lehigh University, Bethlehem, PA 18015 USA. X. Yuan can be contacted at (610) 758-5109 or xiy2@lehigh.edu.

C. Goldsmith is with MEMtronics Corporation, Plano, TX 75075 USA.

C. Nordquist and C. Dyck are with Sandia National Laboratories, Albuquerque, NM 87185 USA.

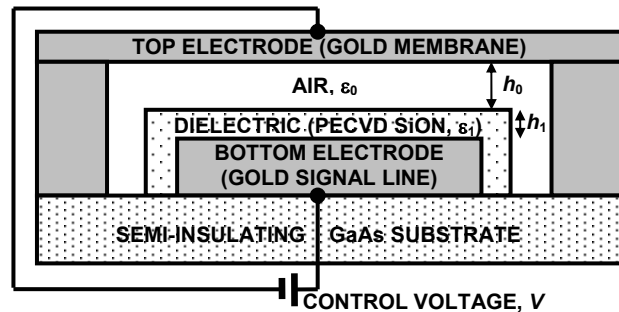


Fig. 1. Cross section (not to scale) of a MEMS capacitive switch.

II. EXPERIMENTAL

Fig. 1 illustrates the metal-dielectric-metal capacitive switches fabricated on GaAs [3]. The dielectric is PECVD silicon oxynitride with a thickness of $0.22 \mu\text{m}$ and a dielectric constant of 5.7. Both the top and bottom electrodes are made of gold. The top electrode is a $1.2\text{-}\mu\text{m}$ -thick flexible membrane that is grounded. The bottom electrode serves as the center conductor of a 50Ω coplanar waveguide for the RF signal. Without any electrostatic force, the membrane is normally suspended in air $4 \mu\text{m}$ above the dielectric. Control voltage is applied to the bottom electrode, which brings the membrane in contact with the dielectric. This forms a large ($260 \mu\text{m} \times 100 \mu\text{m}$) capacitor, which causes the RF signal to be shunted to ground. Without the control voltage, the membrane is supposed to spring back to its fully suspended position, resulting in little capacitive load to the RF signal.

Electrical stress experiments were conducted through either repeated sweeping or continuous application of control voltage on the bottom electrode, then monitoring their effects on capacitance-voltage (C - V) and RF-output characteristics. C - V characteristics were calculated (without subtracting parasitic capacitances) from S -parameters measured at 1 GHz while the control voltage was swept from 0 to ± 30 V at a rate of 0.5 V/s. RF output characteristics were measured under a 500 Hz, -20 to 20 V triangular control voltage. The RF input is a 10 GHz, 10 dBm, 2 V peak-to-peak sinusoidal signal. The RF output was sensed by using a 26.5 GHz diode

detector. Both the control and output waveforms were monitored by using an oscilloscope [1].

III. THEORETICAL ANALYSIS

Assuming the switch behaves like a parallel-plate capacitor, the capacitance per unit area of the switch is

$$C = \frac{\varepsilon_0 \varepsilon_1}{\varepsilon_0 h_1 + \varepsilon_1 h_0} \quad (1)$$

where ε_0 is the permittivity of air, ε_1 is the permittivity of silicon oxynitride, h_0 is the air gap, and h_1 is the dielectric thickness. Assuming a sheet charge ρ_S is developed in the dielectric, the unit-area electrostatic force F on the membrane under a control voltage V is

$$F = \frac{\varepsilon_0}{2} \left\{ \frac{V - \frac{(h_1 - \Delta h_1) \rho_S}{\varepsilon_1}}{\frac{1}{\varepsilon_1} [\varepsilon_0 h_1 + \varepsilon_1 (h_0 - \Delta h_0)]} \right\}^2 \quad (2)$$

where Δh_0 is the deflection of the membrane from its fully suspended position, and Δh_1 is the distance between the charge centroid and the top surface of the dielectric. Thus the control-voltage drift due to dielectric charging is

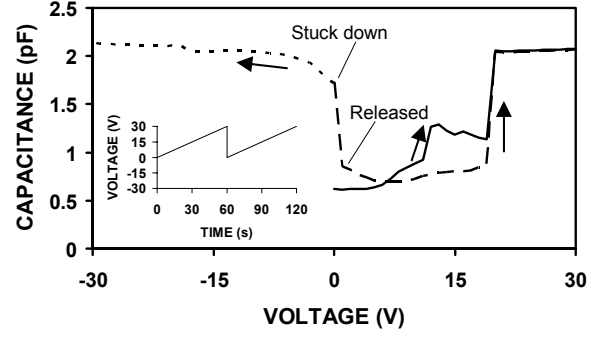
$$\Delta V = \frac{(h_1 - \Delta h_1) \rho_S}{\varepsilon_1} \quad (3)$$

The closer the charge is to the top surface of the dielectric, the greater the effect it has on the control voltage, especially the hold-down voltage.

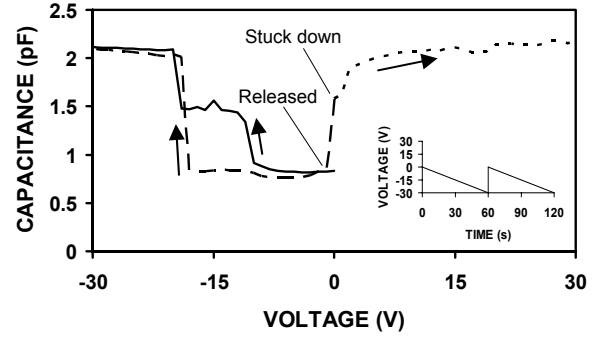
By equating the electrostatic forces of both the control voltage and the dielectric charge to the restoring spring force of the membrane, the control voltage as a function of deflection is

$$V(\Delta h_0) = \frac{1}{\varepsilon_1} \sqrt{\frac{2k\Delta h_0}{\varepsilon_0 A} [\varepsilon_0 h_1 + \varepsilon_1 (h_0 - \Delta h_0)]} + \frac{(h_1 - \Delta h_1) \rho_S}{\varepsilon_1} \quad (4)$$

where k is the spring constant and A is the area of the capacitor. Assuming $\varepsilon_1 (h_0 - \Delta h_0) \gg \varepsilon_0 h_1$, $V(\Delta h_0)$ peaks at $\Delta h_0 \approx h_0/3$ and $V(h_0/3) \approx V_P$ the pull-down voltage [4]. Assuming linear spring action, the spring force when the membrane is all the way down is approximately three times of that at pull down. Therefore, the electrostatic force required to hold down the membrane should be at least three times of the pull-down force. However, the hold-down voltage $V_H \approx V(h_0)$ is much smaller than V_P because $\varepsilon_1 h_0 \gg \varepsilon_0 h_1$. Assuming $V_P = 10$ V, the corresponding pull-down force per unit area is 61 N/m² according to (2). When the membrane is all the way down, a sheet charge as small as $\rho_S = 7.5 \times 10^{10}$ /cm² in the middle of the dielectric can generate an unit-area attraction force of 200 N/m², which should be sufficient to hold down the membrane without any control voltage applied. By contrast, the same amount of sheet charge will only reduce the pull-down force by 5%. Therefore, the above analysis suggests that dielectric



(a)



(b)

Fig. 2. (a) Comparison of (—) pristine and post-stress C - V sweep from (---) 0 to 30 V and (•••) from 0 to -30 V. The stress was applied through repeated 0 to 30 V sweeps. (b) Comparison of (—) pristine and post-stress C - V sweep from (---) 0 to -30 V and (•••) from 0 to 30 V. The stress was applied through repeated 0 to -30 V sweeps. Arrows indicate sweep directions. Sweep rate = 0.5 V/s.

charging can have a greater impact on the hold-down force than on the pull-down force.

IV. RESULTS AND DISCUSSION

Fig. 2(a) compares C - V characteristics before and after positive voltage stress by repeated sweeps to 30 V. Before stress, the switch partially actuates at ~ 10 V with full actuation occurring at ~ 20 V. We believe such a partial actuation is due to relatively rapid negative charging of the dielectric, which causes V_P to increase within an actuation cycle. With repeated sweeps, partial actuation gradually disappears and V_P is consistently ~ 20 V, which suggests that this relatively rapid charging mechanism has become saturated. Meanwhile, the membrane becomes stuck at the beginning of the sweep and is released only at a small positive voltage (~ 1 V). A one-time negative sweep to -30 V on the stressed device causes the membrane to be positively charged and stick harder, which confirms negative charging of the dielectric.

Negative voltage stress at -30 V on the same switch would eventually bleed off the negative charge and cause the dielectric to be positively charged. Fig. 2(b)

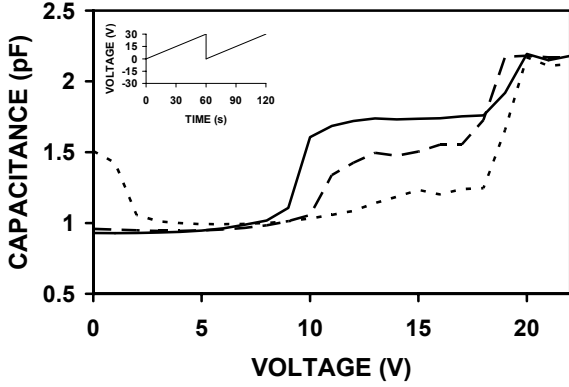
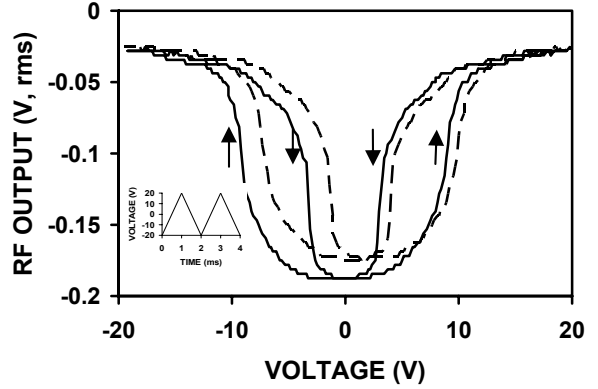


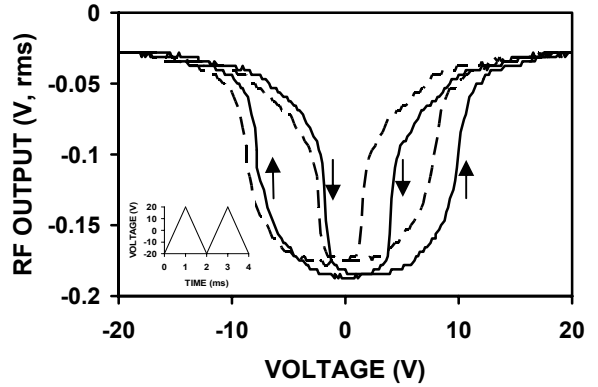
Fig. 3. (—) First, (---) second, and (•••) third C - V measurements of another switch with gradual disappearance of partial actuation and appearance of stiction.

shows that, after repeated negative voltage stress of the same switch, a small negative voltage (-1 V) was required to release the membrane and positive voltage sweep to 30 V only made the stiction worse. Both positive and negative charging could be repeatedly achieved by stressing the switch with negative and positive voltages, respectively, which confirms the amphoteric nature of traps in the dielectric [2]. Storage in room ambient for more than a day would also bleed off the trapped charge and allow partial actuation to reoccur as illustrated in detail in Fig. 3.

When the sweep rate of control voltage is increased from 0.016 Hz to 500 Hz (the control voltage waveform is also changed from saw-tooth to triangular as shown by the insets of Fig. 2, Fig. 3 and Fig. 4) for RF output characterization, partial actuation is not seen from the beginning and V_p is well defined within each actuation cycle. Fig. 4 shows the measured RF output characteristics under a constant-voltage stress of either $+20$ or -20 V. The control voltage, which sweeps from -20 to 20 V in 500 Hz cycles, is plotted on the horizontal axis. The root-mean-square average of the 10 GHz RF output signal, as rectified by the detector diode, is plotted on the vertical axis. The higher the RF output, the more negative the diode voltage. The right side of Fig. 4(a) shows that, initially, under a positive swing of control voltage, $V_p^+ \approx 10$ V while $V_H^+ \approx 4$ V (V_p^+ and V_p^- are V_p under positive and negative swings, respectively. V_H^+ and V_H^- are V_H under positive and negative swings, respectively). Such a hysteresis loop reflects the disparity between the pull-down and hold-down voltages as discussed in Sec. III. Notice that $V_p^+ \approx 10$ V corresponds to the control voltage that causes the initial partial actuation in C - V measurements as shown in Fig. 2 and Fig. 3. Under a negative swing of the control voltage, $V_p^- \approx -V_p^+$ and $V_H^- \approx -V_H^+$, thus forming another loop on the left side of Fig. 4(a) that mirrors the right loop. The symmetry of the two loops about $V = 0$ indicates little charging to begin with.



(a)



(b)

Fig. 4. RF output characteristics under 500 Hz, -20 to 20 V triangular actuation. (a) (—) Before and (---) after 2 minutes of 20 V stress. Negative charging causes the loops to shift right. (b) (—) Before and (---) after 2 minutes of -20 V stress. Positive charging causes the loops to shift left. Arrows indicate voltage sweep direction.

After 2 minutes of constant 20 V stress, both the right and left loops shift to the right indicating negative charging. The shift of the left loop is greater than that of the right loop, which is difficult to explain according to the simple analysis of (2). A possible explanation is that, during the negative swing of control voltage, part of the negative charge in the dielectric migrates toward the top surface making its effect more prominent. The same charge would migrate toward the bottom electrode under the positive swing of the control voltage making its effect less prominent. With prolonged stress under constant 20 V, $V_H^- > 0$ and stiction similar to that observed in C - V measurements occurs. Fig. 4(b) shows the counterpart of Fig. 4(a) for which the switch was stressed with -20 V for 2 minutes. In this case, the loops shift to the left due to positive charging, the shift of the right loop being greater than the shift of the left loop. Therefore, RF output characterization not only confirms charge injection in minutes, but also suggests charge migration in milliseconds in the dielectric.

Another stress effect that is difficult to explain is that the on-state RF output decreases with stress while the off-state RF output remains the same. It is reflected in Fig. 4 as the bottom of the “U” shaped curves moves up with stress while the top stays anchored. This suggests that the membrane is slightly deflected even when it is supposed to be fully up. Simple plastic deformation is ruled out as the RF output recovers to its original level after the switch is stored under room ambient for more than a day. This effect is probably due to lateral variation of dielectric charging or some complicated interaction between charging and the mechanical behavior of the membrane.

The present analysis is based on the simple assumption of a parallel-plate capacitor. In reality, with $V = V_p$, the membrane may make only a partial contact with the dielectric [5]. With $V > V_p$ the contact area increases hence the associated capacitance. This effect can also be used to explain the partial actuation observed in present C - V measurements. However, it is difficult to use the same effect to explain how, after repeated actuation, the partial actuation disappears and the switch actuates at twice the partial-actuation voltage.

V. CONCLUSION

C - V and RF output characteristics of electrostatically actuated MEMS capacitive switches were measured and analyzed. Dielectric charging caused by charge injection under voltage stress was observed. The amphoteric nature of traps and its effect on switch operation were confirmed under both positive and negative control voltages. Charging effects on pull-down and hold-down voltages were analyzed. A hypothesis of charge injection in minutes and charge migration in milliseconds was proposed to explain real-time and non-symmetrical drift of pull-down and hold-down voltages.

Dielectric charging is a complicated process involving different types of traps with time constants differing by orders of magnitude. The above-observed charging effect is probably one of many charging effects that can impact switch operation and lifetime. The hypothesized charging mechanism, which occurs relatively rapidly, is not likely the charging mechanism that prevents the switch from lasting for billions of cycles. It is only through systematic investigation of dielectric-charging effects under different sweep voltages, rates, times and temperatures, as well as full understanding of the charging mechanisms, that accelerated life tests can be conducted under proper stress conditions to determine the mechanism that limits the lifetime of the switches.

ACKNOWLEDGMENT

This work was supported in part by the U.S. Army Research Office and U.S. Army Research Laboratory

and was accomplished under Cooperative Agreement Number DAAD19-02-2-0030. Sandia National Laboratories is a multiprogram laboratory operated by Sandia Corporation, a Lockheed Martin Company, for the United States Department of Energy’s National Nuclear Security Administration under contract DE-AC04-94AL85000.

REFERENCES

- [1] C. Goldsmith, J. Ehmke, A. Malczewski, B. Pillans, S. Eshelman, Z. Yao, J. Brank, and M. Eberly, "Lifetime characterization of capacitive RF MEMS switches," in *Dig. IEEE Int. Microwave Symp.*, 2001, pp. 227-230.
- [2] D. T. Krick, P. M. Lenahan, and J. Kanicki, "Electrically active point defects in amorphous silicon nitride: An illumination and charge injection study," *J. Appl. Phys.*, vol. 64, no. 7, pp. 3558-3563, Oct. 1988.
- [3] C. D. Nordquist, A. Muyschondt, M. V. Pack, P. S. Finnegan, C. W. Dyck, I. C. Reines, G. M. Kraus, G. W. Sloan, and C. T. Sullivan, "MEMS high-Q tunable capacitor for reconfigurable microwave circuits," in *Proc. SPIE 4981*, 2003, pp. 1-8.
- [4] P. M. Zavracky, S. Majumder, and N. E. McGruer, "Micromechanical switches fabricated using nickel surface micromachining," *IEEE J. Microelectromechanical Systems*, vol. 6, pp. 3-9, Mar. 1997.
- [5] E. K. Chan, K. Garikipati, and R. W. Dutton, "Characterization of contact electromechanics through capacitance-voltage measurements and simulations," *IEEE J. Microelectromechanical Systems*, vol. 8, no. 2, pp 208-217, June 1999.